

# Forward modeling-free full waveform inversion with well calibration

Marcelo Guarido\*, Laurence R. Lines\*, Robert J. Ferguson†

## ABSTRACT

Full waveform inversion (FWI) has the goal to find the Earth's model parameters that minimize the difference of acquired and synthetic shots. It is a powerful tool to automatize some complex processes. However, when we talk about seismic data, we are talking about huge datasets, and the FWI shows to be very hard to be applied in large scale, as it requires a large number of synthetic data and migrations at each iteration. In this work, We are proposing an approximation for the FWI that is forward modeling-free, requiring only the migration of the acquired data, which can be pre or post stack, and the optimization driven by a sonic log calibration. We tested the approximation for acoustic inversion in a synthetic 2D Marmousi survey. It is stable and leads to detailed inverted models with reduced computational costs.

## INTRODUCTION

Seismic inversion techniques are the ones that use intrinsic informations contained in the data to determine rock properties by matching a model that "explains" the data. Some examples are the variation of amplitude per offset, or AVO (Shuey, 1985; Fatti et al., 1994), the traveltime differences between traces, named traveltime tomography (Langan et al., 1984; Bishop and Spongberg, 1984; Cutler et al., 1984), or even by matching synthetic data to the observed data, as it is done in full waveform inversion (Tarantola, 1984; Virieux and Operto, 2009; Margrave et al., 2010; Pratt et al., 1998), among others. These inversions can compute rock parameters as P and S waves velocities, density, viscosity and others. In this work I am focused in the inversion of the P wave velocity.

FWI is a least-square based inversion, which objective is to find the model parameters that minimizes the difference between observed (acquired) and synthetic shots (Margrave et al., 2011), or the residuals. This is accomplished in an iterative fit method by linearizing a non-linear problem. It is an algorithm similar to a *Ridge Regression* (Chipman, 1999), which minimizes non-linear problems by adding a regularization term to avoid over fitting (to smooth the model). In seismic processing, I regularize the inversion by convolving the model with a 2D Gaussian window (Margrave et al., 2010).

The full waveform inversion was proposed in the early 80's (Pratt et al., 1998) but the technique was considered too expensive in computational terms. Lailly (1983) and Tarantola (1984) simplified the methodology by using the steepest-descent method (or gradient method) in the time domain to minimize the objective function without calculate, explicitly, the partial derivatives. They compute the gradient by a reverse-time migration (RTM) of the residuals. Pratt et al. (1998) develop a matrix formulation for the full waveform inver-

---

\*CREWES - University of Calgary

†University of Calgary

sion in the frequency domain and present more efficient ways to compute the gradient and the inverse of the Hessian matrix (the sensitive matrix) the Gauss-Newton or the Newton approximations. The FWI is shown to be more efficient if applied in a multi-scale method, where lower frequencies are inverted first and is increased as more iterations are done (Pratt et al., 1998; Virieux and Operto, 2009; Margrave et al., 2010). An overview of the FWI theory and studies are compiled by Virieux and Operto (2009). Lindseth (1979) showed that an impedance inversion from seismic data is not effective due to the lack of low frequencies during the acquisition but could be compensated by the match with a sonic-log profile. Warner and Guasch (2014) use the deviation of the Weiner filters of the real and estimated data as the object function with great results. Margrave et al. (2010) and Romahn and Innanen (2016) calibrate the gradient by matching it with sonic logs, estimating a more precise step length and avoiding cycle skipping. They also use the Gazdag and Sguazzero (1984) PSPI migration algorithm with a deconvolution imaging condition (Margrave et al., 2011; Wenyong et al., 2013) to migrate the residuals faster than the RTM, but preserving the gradient's resolution. Guarido et al. (2015) use the PSPI migration to migrate each frequency content of the residuals independently, generating a pseudo-gradient for each frequency and then averaging stacking them, using the step length as weight. It resulted on a highly detailed model, but the computation costs are high. Guarido et al. (2016) apply an impedance inversion in the gradient to improve the resolution of the inverted model. Guarido et al. (2016, 2017) propose a simpler approximation for the gradient that does not require any forward modeling. They just apply a PSPI migration on the acquired data and compare the result with the current model. The methodology was also extended for a post-stack depth migration. However, two forward modeling are required to estimate the step length.

In this report, we are combining the forward modeling-free gradient approximation (Guarido et al., 2016, 2017) with the well calibration of the gradient (Margrave et al., 2010; Romahn and Innanen, 2016) to propose a cheap full waveform inversion that is forward modeling-free and that provides a detailed inverted model.

## THEORY

### The steepest-descent method

The objective function of the FWI method is (Tarantola, 1984):

$$C(\mathbf{m}) = \|\mathbf{d}_0 - \mathbf{d}(\mathbf{m})\|^2 = \|\Delta\mathbf{d}(\mathbf{m})\|^2 \quad (1)$$

where  $\Delta d$  is the data residual (the difference between acquired and synthetic shots),  $m$  is the model (in this work, the P-wave velocity) and  $\|\cdot\|$  represents the norm-2 of the array. The minimization is done by calculating the Taylor's expansion of the objective function of the equation 1 around a perturbation  $\delta m$  of the model and taking the derivative equal to zero (Tarantola, 1984; Pratt et al., 1998; Virieux and Operto, 2009). The solution is:

$$\mathbf{m}_{n+1} = \mathbf{m}_n - H_n^{-1} \mathbf{g}_n \quad (2)$$

where  $H$  is the Hessian (or sensitive matrix),  $g$  is the gradient computed by back-propagating the data residual and  $n$  is the  $n$ -th iteration. It is known as the Newton method. For the steepest-descent method, the Hessian matrix can be neglected and be equalized to the identity matrix:

$$\mathbf{m}_{n+1} = \mathbf{m}_n - \alpha_n \mathbf{g}_n \quad (3)$$

where  $\alpha$  is the step length, which can be determined by a line search or a least squares minimization (Pica et al., 1990). At this part, the gradient is understood as the reverse-time migration of the residuals. We can interpret this step and expand its meaning to say that the gradient is equivalent to a pre-stack depth migration of the residuals, and we decided to use a PSPI migration of the residuals with a deconvolution imaging condition (Margrave et al., 2010, 2011; Wenyong et al., 2013; Guarido et al., 2014).

### The forward modeling-free gradient

Computing the gradient requires three very known seismic processing steps: PSDM of the residuals, stacking and impedance inversion. Let's understand those steps as the operators  $M$  for migration,  $S$  for stacking and  $I$  for impedance inversion. Equation 3 can be re-written as:

$$\begin{aligned} \mathbf{m}_{n+1} &= \mathbf{m}_n - \alpha_n \mathbf{g}_n \\ &= \mathbf{m}_n - \alpha_n I \{S [M (\Delta \mathbf{d}(\mathbf{m}_n))]\} \\ &= \mathbf{m}_n - \alpha_n I \{S [M (\mathbf{d}_0 - \mathbf{d}(\mathbf{m}_n))]\} \end{aligned} \quad (4)$$

where  $\Delta \mathbf{d}(\mathbf{m}_n)$  is the  $n$ -th iteration residual  $\mathbf{d}_0 - \mathbf{d}(\mathbf{m}_n)$ ,  $\mathbf{d}_0$  is the acquired data,  $\mathbf{d}(\mathbf{m}_n)$  is the synthetic data of the  $n$ -th iteration and  $\mathbf{m}_n$  is the  $n$ -th iteration inverted model. For simplification and easier visualization, let's set  $\mathbf{d}(\mathbf{m}_n) = \mathbf{d}_n$ . Then equation 4 is:

$$\mathbf{m}_{n+1} = \mathbf{m}_n - \alpha_n I \{S [M (\mathbf{d}_0 - \mathbf{d}_n)]\} \quad (5)$$

Considering the linearity property of the migration operator (see appendix), the acquired and synthetic shots can be migrated separately:

$$\mathbf{m}_{n+1} = \mathbf{m}_n - \alpha_n I \{S [M (\mathbf{d}_0) - M (\mathbf{d}_n)]\} \quad (6)$$

The next step is to use the linearity property of the stacking operator and equation 6 becomes:

$$\mathbf{m}_{n+1} = \mathbf{m}_n - \alpha_n I \{S [M (\mathbf{d}_0)] - S [M (\mathbf{d}_n)]\} \quad (7)$$

For the impedance inversion operator, the first approximation we tried is  $I(x_1 - x_2) = I_0 \frac{I(x_1)}{I(2_2)}$ . Then equation 7 can be written as:

$$\mathbf{m}_{n+1} = \mathbf{m}_n - \alpha_n I_0 \frac{I \{S [M (\mathbf{d}_0)]\}}{\underbrace{I \{S [M (\mathbf{d}_n)]\}}_{\text{Current model}}} \quad (8)$$

where the denominator is the impedance inversion of the stacked depth migrated synthetic shots should be the velocity model on which the forward modeling algorithm is ran into. In others words, it is the model of the current iteration  $\mathbf{m}_n$ . Then equation 11 can be simplified to:

$$\mathbf{m}_{n+1} = \mathbf{m}_n - \alpha_n I_0 \frac{I \{S [M (\mathbf{d}_0)]\}}{\mathbf{m}_n} \quad (9)$$

Equation 9 shows to be unstable as it can be divided by zero (as we are inverting for lower frequencies greater than 3Hz and not capturing the Earth linear trend, it can result on zeros and even negative impedance). Trying to avoid this we added a stabilization factor SF:

$$\mathbf{m}_{n+1} = \mathbf{m}_n - \alpha_n I_0 \frac{I \{S [M (\mathbf{d}_0)]\}}{\mathbf{m}_n + SF} \quad (10)$$

Choosing a value for the stabilization factor showed to be challenging. A too small value can lead areas of the gradient to have a huge value compared with its neighbors. A large value (around 1 and above) can change the denominator significantly. And the value needed to be changed at each iteration by trial and error. Avoiding the division of equation 10 is the best tactic at this point. So we took the risk to say that the impedance inversion operator is *approximately* linear (for that, we assume Earth impedance to follow a linear trend and a Taylor expansion of the reflection coefficients is used to estimate the update as a perturbation of Earth's impedance), we end up with another solution for equation 7:

$$\mathbf{m}_{n+1} = \mathbf{m}_n - \alpha_n (I \{S [M (\mathbf{d}_0)]\} - \underbrace{I \{S [M (\mathbf{d}_n)]\}}_{\text{Current model}}) \quad (11)$$

Again, on the second hand of the gradient approximation we have the model of the current iteration  $\mathbf{m}_n$ . Then equation 11 is simplified to:

$$\mathbf{m}_{n+1} = \mathbf{m}_n - \alpha_n (I \{S [M (\mathbf{d}_0)]\} - \mathbf{m}_n) \quad (12)$$

Equations 12 and 10 understand the gradient as a residual impedance inversion of the acquired data relative to the current model. The objective function is being minimized on

the estimation of the step length, that requires 2 forward modeling when using Pica et al. (1990)'s approximation.

Looking again at equation 12, we understand that we are estimating the gradient by applying some seismic processing tools. If we think about migration and stack, migrating the data and stacking should have the same effect as doing the inverted process (stack then migrate). Then equation 12 is equivalent to:

$$\mathbf{m}_{n+1} = \mathbf{m}_n - \alpha_n (I \{M [S (\mathbf{d}_0)]\} - \mathbf{m}_n) \quad (13)$$

This means I can input in the algorithm a stacked section (figure 1) and apply a post-stack depth migration algorithm (we used a zero-offset based PSPI with a cross-correlation imaging condition). The stacking velocity used is the same initial model of the others tests. However it was converted to a rms velocity..

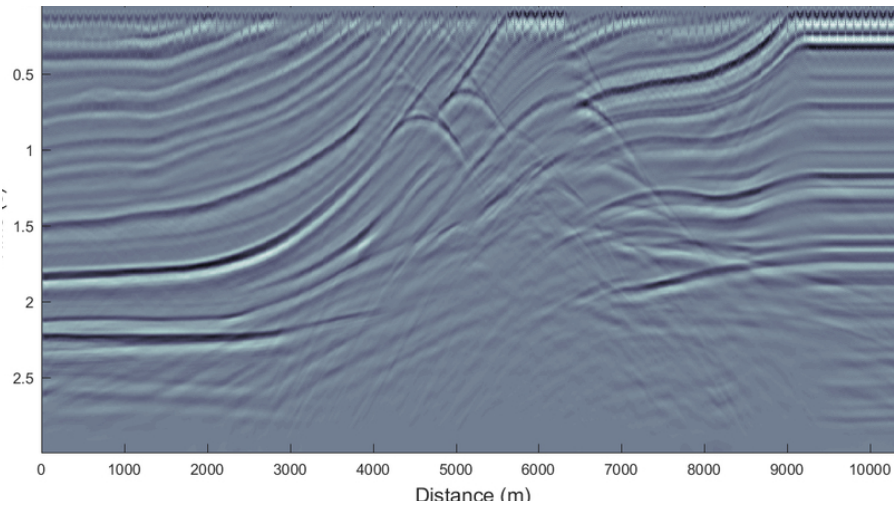


FIG. 1. Stacked section used as input in the post-stack method.

Analyzing the stacked section on figure 1, we noticed the presence of diffractions on the center area of the model caused by the fault zones. We can also observe a strong horizontal event close to the surface and also internal multiples are very evident on the deeper areas. We took note of all those observations and studied how they affected the inversion.

### Well calibration

Until now we are assuming Pica et al. (1990)'s approximation to determine the step length on equations 12 and 13. However, it goes against our seeking for a forward modeling-free routine, as they still require two forward modeling to estimate the step length. Margrave et al. (2010) and Romahn and Innanen (2016) calibrate the gradient by matching it with a sonic log at the same spatial location. They estimate a scalar and phase rotation to create a match filter to convolve with the gradient. This would lead us with a FWI algorithm 100% forward modeling-free. So we decided to implement it.

To find the scalar  $\alpha$  that minimizes the impedance inverted gradient trace  $S_{grad}$  to the impedance (sonic log) well trace  $S_{well}$ , we minimize the L2-norm function for  $\alpha$ :

$$\Phi = ||S_{well} - \alpha S_{grad}||^2 \quad (14)$$

This leads to a simple equation to estimate  $\alpha$ :

$$\alpha = \frac{S_{well}^T S_{grad}}{S_{grad}^T S_{grad}} \quad (15)$$

For the phase rotation, we use the *Toolbox* code *constphase.m* that finds the angle  $\phi$  that makes  $S_{grad}$  look like  $S_{well}$ . By finding  $\alpha$  and  $\phi$ , we create a matching filter which is convolved with the gradient to have the model update.

Combining the well tie calibration with the forward modeling-free gradient of equations 12 and 13, we are proposing a new FWI routine that is 100% forward modeling-free. This reduces significantly the cost of the inversion without the need of the source estimation.

## SIMULATION

### Post-stack approximation with well calibration

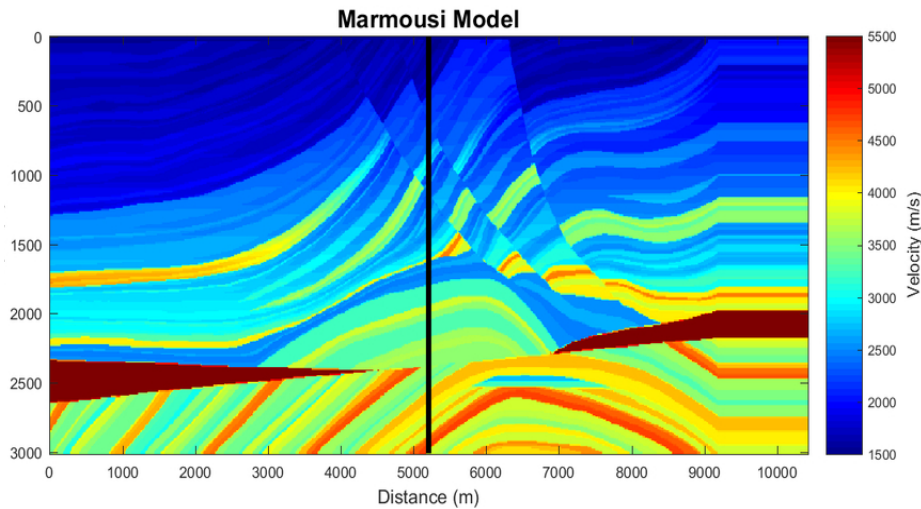


FIG. 2. True Marmousi model. The black line is the well position.

Test are held in the Marmousi model. The well for calibration is selected to be the column in the center of the model, as shown on figure 2.

For the starting model on figure 3, we use a simulation of a velocity analysis output.

The main difference of the routine now is to replace the Pica et al. (1990)'s algorithm to estimate the step length by the well calibration. At each iteration we compute the gradient according to equation 13 and match its central column with the residual well log (the

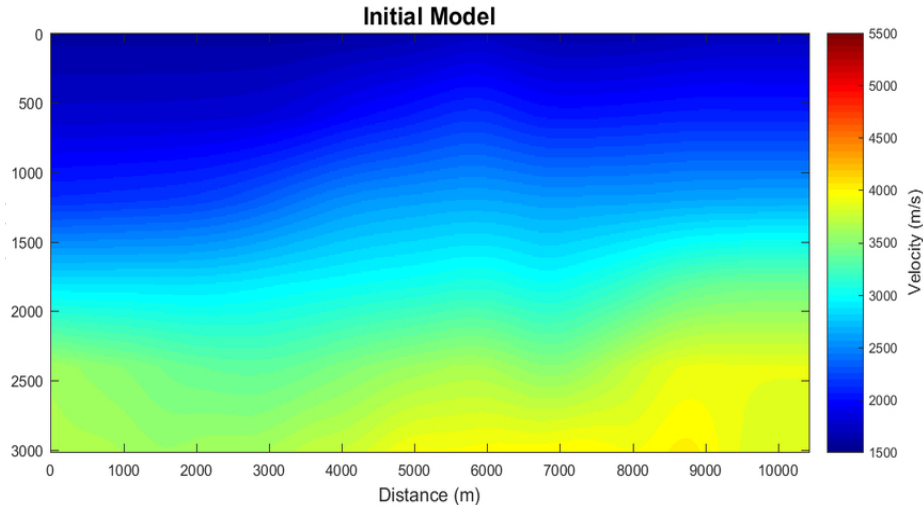


FIG. 3. The initial model is a simulation of a velocity analysis output.

difference of the well and current model). Computes a scale factor and phase rotation to generate a match filter that, by convolving with the gradient, results on a model updated that is optimized in the well location. The frequency content per iteration is a little different than before. Now, for the first iteration, the frequency range to estimate the gradient is from  $4Hz$  to  $9Hz$ . At each iteration, the frequency range is increased by  $1Hz$  until the maximum of  $30Hz$ .

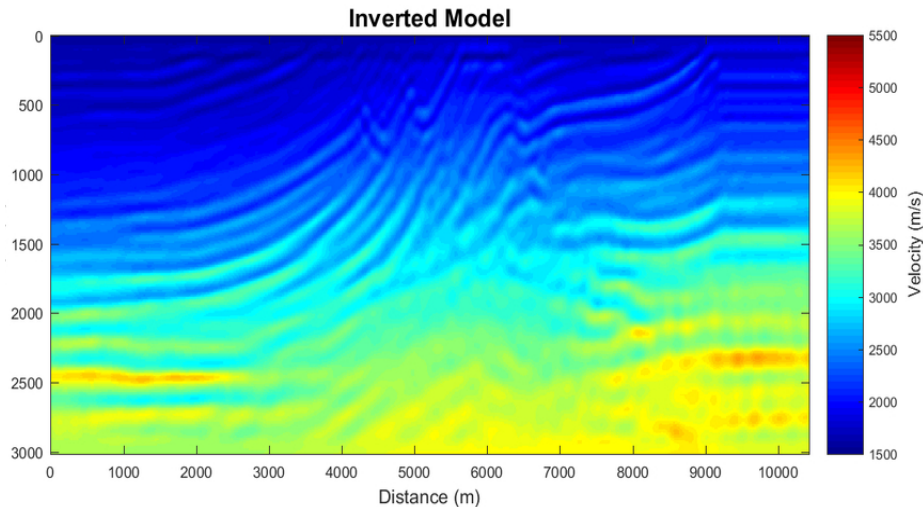


FIG. 4. Inverted model for the post-stack method with well calibration.

After running 25 iterations in 8 minutes on a personal laptop, the inverted model of figure 4 shows impressive resolution (higher resolution than we were expecting) with low cost. All main structures are recovered and even in the deep area of the model, some layers started to show their shape. The three large faults in the central part are also visible and can be used by interpreters. Multiples of the high velocity bodies are present below 2500m depth. However, the most impressive result is the reduced cost to run the routine. As cited previously, it took only 8 minutes to be completed. The band-limited impedance inversion

based gradient of chapter ?? took about 48 hours to complete and it required 48 nodes of the *CREWES* supercomputer. Comparing both ending models, the cost reduction came with some loss in resolution, but models are still comparable.

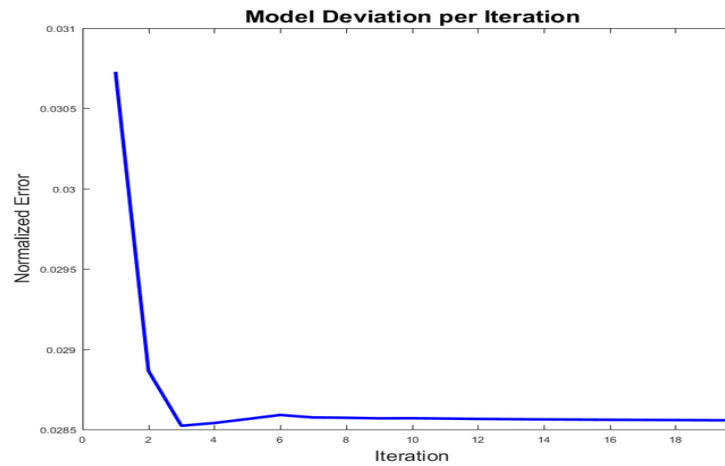


FIG. 5. Model deviation of the post-stack approximation with well calibration. The convergence is fast, reached on the very first iterations.

As any synthetic shot is generated during the process, the objective function is not measured at each iteration. But, as we have the true model, we computed the model deviation per iteration in figure 5 and it is clear that the inversion is stable. The method converges fast, in about 2 iterations. After that there is a small increment in error that is slowly reduced as iterations advance.

### Pre-stack approximation with well calibration

In the previous section, the post-stack method is combined with a well calibration of the gradient, providing a fast solution, with surprising high resolution. Now, we are testing the same method, but with a pre-stack migration. We are losing in cost, but we now, now, seeking improvements in quality.

By using the same starting model of figure 3, the resulted inversion of figure 6 has incredible resolution, improving the resolution of the post-stack method (figure 4). The multiples below 2500m are still visible, but the structures in the central part of the model are more clear. The high velocity bodies are better placed with closer true velocity. Only the shallow portion looks to be blurred, when compared to the post-stack method.

The model deviation of figure 7 shows a fast convergence. Basically, the best fit is reached at the very first iteration. After that the deviation just flies around the minimum.

This model came with some loss in cost, as it took about 6 hours to be completed using a personal laptop. As surveys get larger, with more shot points and recording time, running time will increase as well. So, all is a matter of cost/quality trade-off.

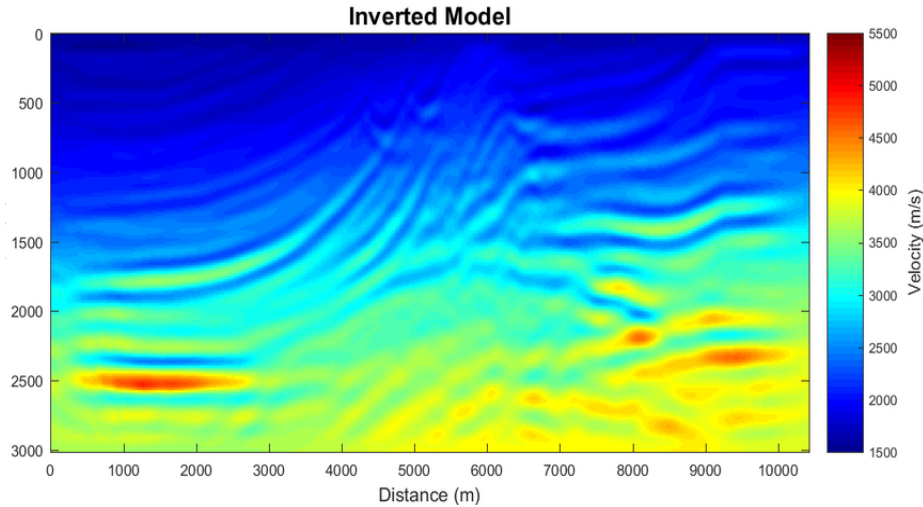


FIG. 6. Inverted model for the post-stack method with well calibration.

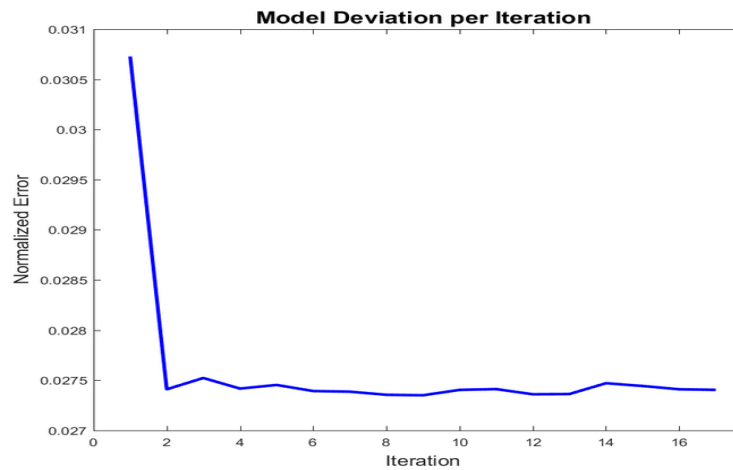


FIG. 7. Model deviation of the pre-stack approximation with well calibration. The inverted model goes closer to the true model.

### Velocity models as migration velocities

It is clear as by applying the FWI routine, the starting model is improved and features of the true model are included to the final inversion. This is very helpful for seismic interpretation. Now, let's remember that, usually, the starting model of the FWI routine is the best migration velocity from the seismic processing. So, we are wondering if the FWI can also improve the subsurface image by providing a better migration velocity. For this analysis, 3 velocities are chosen to migrate the acquired data: the velocity analysis initial model (figure 8a), the post-stack forward modeling-free with well calibration (figure 8c), and the pre-stack forward modeling-free with well calibration (figure 8e). For the pre-stack migration, we use the PSPI migration, with a deconvolution imaging condition, on the acquired data. As the data does not contain higher frequencies, we migrate the data on the frequency band from  $1Hz$  to  $60Hz$ . The migrated shots are muted and stacked to form a subsurface image (figures 8b, 8d and 8f).

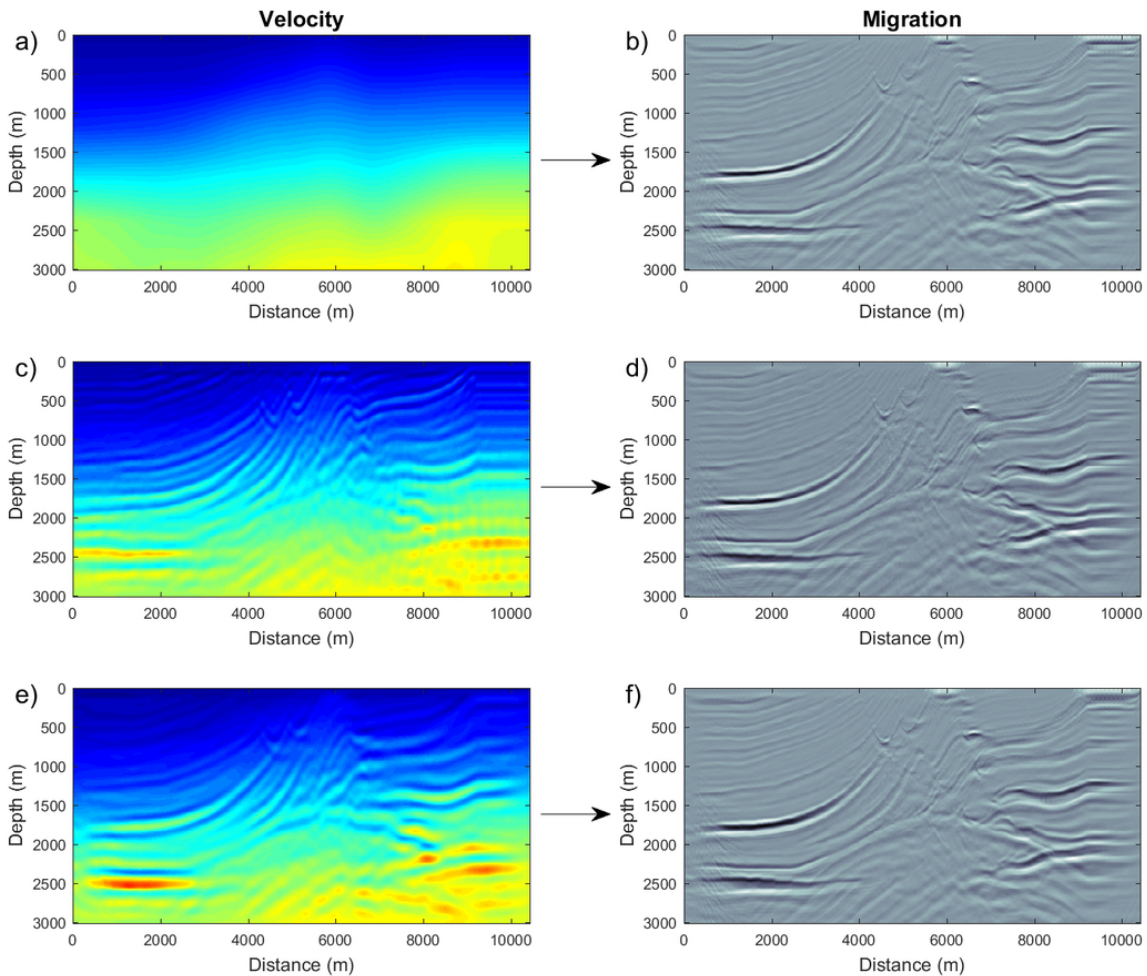


FIG. 8. Using the models a) initial, c) post-stack and e) pre-stack to apply a pre-stack migration of the acquired data and obtain the respective subsurface images b), d) and f). Migration is improved as the model is more precise.

Looking at all the migrated images (figures 8b, 8d and 8f), we can say that all the migration velocities (figures 8a, 8c and 8e) are very similar. Now, looking closely, as we go deeper in the model, structures have different positions. It is more evident at the high velocity body in the left size of the model on the depth of 2500m. The post-stack FWI started to place the structure in a more correct place, as the pre-stack FWI did even a better job. So, the higher resolution the model has, higher the resolution the subsurface image have. And it is more evident as deeper as we go.

We are confident that we are proposing a cheap and fast FWI that will improve the initial model to help in the seismic interpretation of the survey and to provide a clearer subsurface image by providing a more accurate migration velocity.

## CONCLUSIONS

In this work we proposed a new approximation for the full waveform inversion that, assuming linearity of the seismic processing tools, allows us to obtain the gradient free of forward modeling, and combining it with the well calibration of the gradient, replacing the

step length, we have a full waveform inversion that is 100% free of forward modeling and source estimation. We should consider that for an initial model that is far from the true model, both the pre and post stack approximations resulted on inverted models with high level of details, with reduced computing costs. In the future work, we will be extending the same approximation idea for a multi-parameter FWI (if possible) and for 3D seismic surveys.

## ACKNOWLEDGMENTS

The authors thank the sponsors of CREWES for continued support. This work was funded by CREWES industrial sponsors and NSERC (Natural Science and Engineering Research Council of Canada) through the grant CRDPJ 461179-13. We thank Dr. Gary Margrave and Soane Mota dos Santos for the suggestions, tips and productive discussions.

## REFERENCES

- Bishop, T. N., and Spongberg, M. E., 1984, Seismic tomography: A case study: SEG Technical Program Expanded Abstracts, **313**, 712–713.
- Chipman, J. S., 1999, Linear restrictions, rank reduction, and biased estimation in linear regression: Linear Algebra and its Applications, **289**, No. 1, 55 – 74.
- Cutler, R. T., Bishop, T. N., Wyld, H. W., Shuey, R. T., Kroeger, R. A., Jones, R. C., and Rathbun, M. L., 1984, Seismic tomography: Formulation and methodology: SEG Technical Program Expanded Abstracts, **312**, 711–712.
- Fatti, J. L., Smith, G. C., Vail, P. J., Strauss, P. J., and Levitt, P. R., 1994, Detection of gas in sandstone reservoirs using avo analysis: A 3-d seismic case history using the geostack technique: Geophysics, **59**, No. 9, 1362–1376.
- Gazdag, J., and Sguazzero, P., 1984, Migration of seismic data by phase shift plus interpolation: Geophysics, **49**, No. 2, 124–131.
- Guarido, M., Lines, L., and Ferguson, R., 2014, Full waveform inversion - a synthetic test using the pspi migration: CREWES Research Report, **26**, 26.1–26.23.
- Guarido, M., Lines, L., and Ferguson, R., 2015, Full waveform inversion: a synthetic test using pspi migration: SEG Technical Program Expanded Abstract, **279**, 1456–1460.
- Guarido, M., Lines, L., and Ferguson, R., 2016, Fwi without tears: a forward modeling free gradient: CREWES Research Report, **26**, 26.1–26.20.
- Guarido, M., Lines, L., and Ferguson, R., 2017, Fwi without tears: a forward modeling-free gradient: SEG Technical Program Expanded Abstract, 1588–1593.
- Lailly, P., 1983, The seismic inverse problem as a sequence of before stack migrations: Conference on inverse scattering, theory and application: Society of Industrial and Applied Mathematics, Expanded Abstracts, 206–220.
- Langan, R. T., Lerche, I., Cutler, R. T., Bishop, T. N., and Spera, N. J., 1984, Seismic tomography: The accurate and efficient tracing of rays through heterogeneous media: SEG Technical Program Expanded Abstracts, **314**, 713–715.
- Lindseth, R. O., 1979, Synthetic sonic logs-a process for stratigraphic interpretation: Geophysics, **44**, No. 1, 3–26.
- Margrave, G., Ferguson, R., and Hogan, C., 2010, Full waveform inversion with wave equation migration and well control: CREWES Research Report, **22**, 63.1–63.20.

- Margrave, G., Yedlin, M., and Innanen, K., 2011, Full waveform inversion and the inverse hessian: CREWES Research Report, **23**, 77.1–77.13.
- Pica, A., Diet, J. P., and Tarantola, A., 1990, Nonlinear inversion of seismic reflection data in a laterally invariant medium: *Geophysics*, **55**, No. 2, R59–R80.
- Pratt, R. G., Shin, C., and Hick, G. J., 1998, Gauss-newton and full newton methods in frequency-space seismic waveform inversion: *Geophysical Journal International*, **133**, No. 2, 341–362.
- Romahn, S., and Innanen, K., 2016, Immi: the role of well calibration in the context of high geological complexity: CREWES Research Report, **28**, 66.1–66.17.
- Shuey, R. T., 1985, A simplification of the Zoeppritz equations: *Geophysics*, **50**, No. 4, 609–614.
- Tarantola, A., 1984, Inversion of seismic reflection data in the acoustic approximation: *Geophysics*, **49**, No. 8, 1259–1266.
- Virieux, J., and Operto, S., 2009, An overview of full-waveform inversion in exploration geophysics: *Geophysics*, **74**, No. 6, WCC1–WCC26.
- Warner, M., and Guasch, L., 2014, Adaptive waveform inversion: Theory: SEG Technical Program Expanded Abstracts, **207**, 1089–1093.
- Wenyong, P., Margrave, G., and Innanen, K., 2013, On the role of the deconvolution imaging condition in full waveform inversion: CREWES Research Report, **25**, 72.1–72.19.